ENVIRONMENTAL RESEARCH
LETTERS

LETTER • OPEN ACCESS

Forest disturbance alerts for the Congo Basin using Sentinel-1

To cite this article: Johannes Reiche *et al* 2021 *Environ. Res. Lett.* **16** 024005

ENVIRONMENTAL RESEARCH
LETTERS

CrossMark

OPEN ACCESS

RECEIVED
29 July 2020

REVISED
23 November 2020

ACCEPTED FOR PUBLICATION
4 December 2020

PUBLISHED
19 January 2021

LETTER

Forest disturbance alerts for the Congo Basin using Sentinel-1

Johannes Reiche[1,7], Adugna Mullissa[1], Bart Slagter[1], Yaqing Gou[1], Nandin-Erdene Tsendbazar[1], Christelle Odongo-Braun[1], Andreas Vollrath[2], Mikaela J Weisse[3], Fred Stolle[3], Amy Pickens[4], Gennadii Donchyts[5], Nicholas Clinton[6], Noel Gorelick[6] and Martin Herold[1]

1 Wageningen University, Wageningen, The Netherlands
2 European Space Agency, ESRIN, Frascati, Italy
3 World Resources Institute, Washington DC, United States of America
4 University of Maryland, College Park, MD, United States of America
5 Deltares, Delft, The Netherlands
6 Google, Mountain View, CA, United States of America
7 Author to whom any correspondence should be addressed.

E-mail: johannes.reiche@wur.nl

Keywords: forest disturbance alerts, Congo Basin, humid tropical forest, deforestation, near real-time, Sentinel-1, radar

Abstract

A humid tropical forest disturbance alert using Sentinel-1 radar data is presented for the Congo Basin. Radar satellite signals can penetrate through clouds, allowing Sentinel-1 to provide gap-free observations for the tropics consistently every 6–12 days at 10 m spatial scale. In the densely cloud covered Congo Basin, this represents a major advantage for the rapid detection of small-scale forest disturbances such as subsistence agriculture and selective logging. Alerts were detected with latest available Sentinel-1 images and results are presented from January 2019 to July 2020. We mapped 4 million disturbance events during this period, totalling 1.4 million ha with nearly 80% of events smaller than 0.5 ha. Monthly distribution of alert totals varied widely across the Congo Basin countries and can be linked to regional differences in wet and dry season cycles, with more forest disturbances in the dry season. Results indicated high user's and producer's accuracies and the rapid confirmation of alerts within a few weeks. Our disturbance alerts provide confident detection of events larger than or equal to 0.2 ha but do not include smaller events, which suggests that disturbance rates in the Congo Basin are even higher than presented in this study. The new alert product can help to better study the forest dynamics in the Congo Basin with improved spatial and temporal detail and near real-time detections, and highlights the value of dense Sentinel-1 time series data for large-area tropical forest monitoring. The research contributes to the Global Forest Watch initiative in providing timely and accurate information to support a wide range of stakeholders in sustainable forest management and law enforcement. The alerts are available via the https://www.globalforestwatch.org and http://radd-alert.wur.nl.

1. Introduction

The Congo Basin rainforest is the second-largest in the world, covering almost 200 million ha of humid tropical forest. It plays a crucial role in the global climate cycle and provides local livelihoods and resources for more than 100 million people across six countries: Cameroon, Central African Republic, the Democratic Republic of the Congo, Equatorial Guinea, Gabon and the Republic of the Congo (Somorin *et al* 2012). Despite its importance, forest dynamics in the Congo Basin remain understudied compared to those in Amazon and Southeast Asian rainforests, and it is only recently that scientists have begun to systematically evaluate how and why Congo Basin forests are changing (Tyukavina *et al* 2018, Creese *et al* 2019, Kleinschroth *et al* 2019).

The rapidly growing population in the Congo Basin has led to an acceleration of forest disturbance rates over the past decades, with an estimated 16 million ha of forest cleared between 2000 and 2014 (Tyukavina *et al* 2018). Smallholder agriculture causes the large majority of forest disturbances. Other major drivers include selective logging, mining, and road expansion (Potapov *et al* 2012, Tyukavina *et al* 2018, Umunay *et al* 2019). Artisanal and industrial logging account for 10% of the total forest disturbance across the Congo Basin, but up to 60% in individual countries, such as Gabon (Tyukavina *et al* 2018). A large part of the forest disturbances in the Congo Basin is considered unsustainable and/or illegal (Lescuyer *et al* 2014, Kleinschroth *et al* 2019, Umunay *et al* 2019).

In the past 10 years, satellite-based alert systems (Diniz *et al* 2015, Hansen *et al* 2016, Watanabe *et al* 2018) have emerged as the primary tool to provide near real-time information on newly disturbed tropical forest areas. A wide range of stakeholders, including governments, NGOs, private sector actors and communities across the tropics have recognized the value of satellite-based disturbance alert products to empower sustainable land management and law enforcement actions against illegal forest activities (Lynch *et al* 2013, Finer *et al* 2018, Weisse *et al* 2019, Tabor and Holland 2020). Open distribution and availability of key forest disturbance alerts via nationally-hosted web portals and the World Resources Institute's Global Forest Watch platform have led to further increases in transparency of ongoing forest activities globally (Finer *et al* 2018, Tabor and Holland 2020).

Current operational systems rely predominantly on freely available medium scale resolution (30–100 m) optical satellite data (Souza *et al* 2009, Diniz *et al* 2015, Hansen *et al* 2016, Vargas *et al* 2019). The Brazilian Real-Time System for Detection of Deforestation uses data from the Advanced Wide Field Sensor onboard the Indian Remote Sensing satellites and provides monthly forest disturbance information at 56 m spatial scale (Diniz *et al* 2015). Other operational systems use medium resolution Landsat data to provide pixel-based disturbance alerts at 30 m scale, including the Peruvian Geobosques system (Vargas *et al* 2019) and the Global Land Analysis and Discovery (GLAD) pan-tropical forest disturbance alerts (Hansen *et al* 2016). The limited availability of cloud-free Landsat data in many parts of the humid tropics reduces the ability to track forest change events consistently on a near real-time basis (Souza *et al* 2013, Sannier *et al* 2014, Hansen *et al* 2016). In the Congo Basin, cloud-free observations are rare during the wet season in particular. In persistently cloud covered regions such as the western part of the Congo Basin, cloud-free Landsat observations can be more than 1 year apart (Sannier *et al* 2014, Hansen *et al* 2016, Tyukavina *et al* 2018).

In addition to preventing detection of disturbances in near real-time, long data gaps also represent a major challenge for detecting small-scale changes. After selective logging, for example, any sign of disturbance within remotely sensed data often disappears within weeks or months due to fast regeneration, canopy closure and understory revegetation (figure 1) (Asner *et al* 2004, Souza *et al* 2005, Verhegghen *et al* 2015). Disturbances at the scale of a single tree canopy are unlikely to be captured by a 30 m Landsat alert regardless of cloud-free observation availability and require finer scale satellite data (Verhegghen *et al* 2015).

Satellite-based high-resolution radar sensors use long-wavelength energy that penetrates through clouds and smoke and is sensitive to changes in the physical structure of forests, resulting in major advantages for tropical forest disturbance monitoring (Joshi *et al* 2016, Reiche *et al* 2016). In the past, inconsistent data acquisitions and commercial data distribution of key radar missions restricted opportunities for operational large-scale forest monitoring (Reiche *et al* 2016). New and near-future radar satellites now provide a wealth of free, consistent radar data for global forest monitoring (Reiche *et al* 2016). For example, the JiCA-JAXA Forest Early Warning System in the Tropics (JJ-FAST) employs long-wavelength ALOS-2 PALSAR-2 L-band radar data with a spatial scale of 50 m, and provides event-based forest disturbance detection for the pan-tropics updated every 1.5 months (Watanabe *et al* 2018). A minimum event area size of 2 ha (version 3), however, limits the capacities of the JJ-FAST system to detect small-scale changes.

With the European Sentinel-1A and 1B C-band radar satellites launched in 2014 and 2016 (Torres *et al* 2012), global temporally dense and high resolution radar data at 10 m spatial scale are freely available for the first time. While the majority of the tropics, including the Congo Basin, is consistently covered every 12 days by one ascending or one descending orbit, tectonically and volcanically active regions such as western South America, East Africa and parts of South East Asia are covered every 6 days (Potin *et al* 2016). Compared to long-wavelength L-band (∼23 cm) radar, short wavelength C-band (∼5.6 cm) radar is considered less suitable for forest change monitoring because of the rapid saturation of the signal over forests, and the higher sensitivity to surface moisture fluctuations (Ulaby *et al* 1986). A number of recent studies, however, have shown that the dense observation frequency of Sentinel-1 in combination with high spatial resolution can overcome major shortcomings of C-band radar and have demonstrated the potential of Sentinel-1 for accurate and timely tracking of small-scale forest disturbance, including selective logging (Bouvet *et al* 2018, Reiche *et al* 2018b, Ballère *et al* 2021, Hethcoat *et al* 2020, Hirschmugl *et al* 2020, Hoekman *et al* 2020).

Here we present a Sentinel-1-based forest disturbance alert system deployed and validated for the humid tropical forest of the Congo Basin. The system is implemented in Google Earth Engine (Gorelick *et al* 2017), and developed in collaboration with World Resource Institute's Global Forest Watch program and Google.

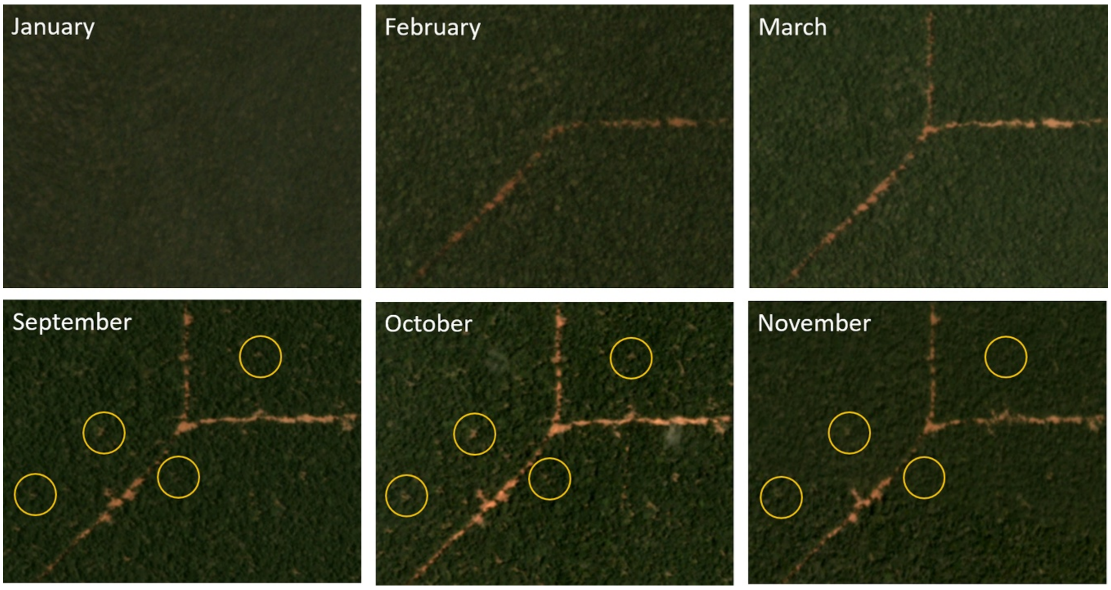

Figure 1. Logging road expansion (January, February, March) followed by selective logging (September and October) and rapid canopy closure (November), depicted by monthly PlanetScope imagery with a spatial resolution of 3 m (Planet Team 2020). Circles indicate canopy openings after logging (October) and canopy closure within one to two months (November). Location: Sangha-Mbaéré district, Central African Republic (center coordinate: 3.95° N, 15.99° E).

2. Study area and definitions

We defined the study area as humid tropical forest within the six Congo Basin countries (figure 2A). The climate in the Congo Basin countries is warm and humid with mean annual temperatures between 24 °C and 26 °C and mean annual rainfall between 1400 and 2200 mm (Harris *et al* 2014).

We used the global forest change products (version 1.7) developed by Hansen *et al* (2013) to derive a benchmark forest map for the year 2018 which we used to limit the detection of new disturbance alerts to undisturbed humid tropical forest at the beginning of our monitoring in 2019. We used the year 2000 tree canopy cover product with a threshold of >50% tree canopy cover and excluded all historic forest loss from 2000 to 2018 (Hansen *et al* 2013). The evergreen forest layer of the Collection 2 Copernicus Global Land Cover dataset (Buchhorn *et al* 2020) was used to exclude dry tropical forests. We further refined and removed errors from the map with the aid of a radar-based global forest map (Martone *et al* 2018). Our forest benchmark map covered 186 115 kha (1 kha = 1000 ha) humid tropical forest area (figure 2A).

We defined forest disturbance as the complete or partial removal of tree cover within a 10 m × 10 m Sentinel-1 pixel (∼0.01 ha). Complete tree cover removal is associated with stand-replacement disturbance at the Sentinel-1 pixel scale, while partial removal mainly represents disturbances associated with boundary pixels and selective logging. This definition is similar to other operational satellite-based forest change products (Hansen *et al* 2013, 2016, Vargas *et al* 2019).

We applied a conservative minimum mapping unit of 0.2 ha (20 Sentinel-1 pixels, 2.2 Landsat pixels) as we aimed for an alert with a low false detection rate. Mapping very fine-scale disturbance events covering few Sentinel-1 pixels is naturally associated with increasing false detection rates, for example due to remaining speckle noise or local moisture fluctuations (Bouvet *et al* 2018, Reiche *et al* 2018b, Hirschmugl *et al* 2020).

Our alert is a generic one for detecting forest disturbances. We do not distinguish human-induced from natural forest disturbances, similar to other forest disturbance alerting products (Hansen *et al* 2016, Watanabe *et al* 2018). Natural disturbances may include windthrows, landslides, or meandering rivers.

3. Sentinel-1 satellite data

We employed dual-polarized (VV and VH) high resolution Sentinel-1 Ground Range Detected (GRD) products acquired in interferometric wide swath and available in the Google Earth Engine collection (Google Earth Engine 2020).

The GRD images have a pixel spacing of 10 m at which the full information detail is guaranteed, and a spatial resolution, i.e. the ability to separate between adjacent target objects on the ground, of approximately 20 m × 22 m (European Space Agency 2020a). In this study, GRD images acquired in ascending and descending orbits were considered (figure 2B), which corresponded to an annual total of approximately 5300 images. For the period between January 2019 and July 2020, 72% of the benchmark forest map was covered every 12 days, 21% every 6 days, 7% less than 6 days, and 0.28% was not covered.

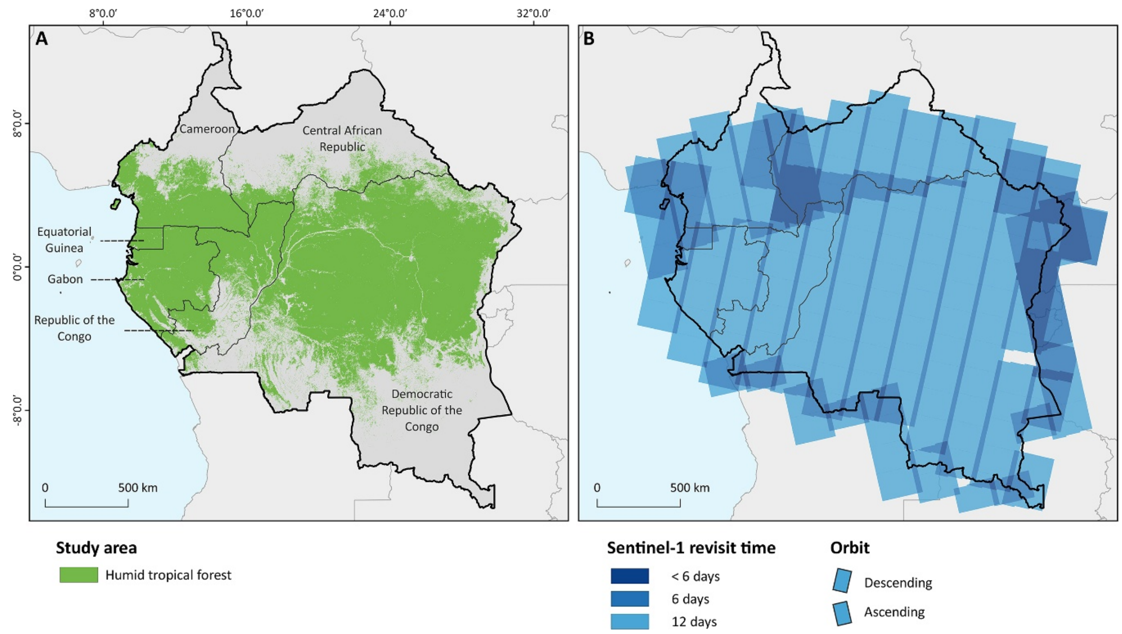

Figure 2. (A) Year 2018 benchmark forest map of the Congo Basin's humid tropical forest. (B) Sentinel-1 data coverage and revisit times for 2019 to 1 July 2020.

4. Methods

4.1. Sentinel-1 data processing

Sentinel-1 GRD images available in the Google Earth Engine collection (Google Earth Engine 2020) have already undergone pre-processing using the European Space Agency's Sentinel-1 Toolbox (European Space Agency 2020b). This includes the application of the orbit files, thermal noise and GRD border noise removal, radiometric calibration to sigma naught, and range-Doppler terrain correction. We applied additional pre-processing steps to further enhance the data, including removing remaining GRD border noise and artefacts occasionally caused by heavy convective rain cells (Danklmayer *et al* 2009) as well as applying radiometric slope correction (Hoekman and Reiche 2015, Vollrath *et al* 2020) and adaptive speckle filtering (Quegan and Yu 2001). The final output was geocoded and topographically normalized gamma-naught VV- and VH-polarized backscatter images at 10 m pixel spacing.

We generated historical time-series metrics of backscatter using all Sentinel-1 GRD images available for 2017 and 2018, including the median and standard deviation derived individually for ascending and descending orbits and VV- and VH-polarization. The time-series metrics were used to describe the backscatter distribution of stable forest at the pixel level (Reiche *et al* 2018b). We assumed that all observations in the 2 year historical period represented stable forest and did not consider possible changes or regrowth processes.

4.2. Sentinel-1-based forest disturbance detection

In our system, a forest disturbance alert is triggered based on a single observation from the latest Sentinel-1 image. Subsequent observations are used to increase confidence and confirm or reject the alert. The date of the alert is set to the date of the image that first triggered the alert (Reiche *et al* 2015, 2018b).

Figure 3 depicts the flowchart of the presented Sentinel-1-based forest disturbance alerting method. The latest Sentinel-1 GRD image was accessed via Google Earth Engine. Quality control, radiometric slope correction and speckle filtering were applied (see section 4.1) before we normalized the image by matching the median backscatter distribution of forest to the expected median distribution defined by the historical time-series metrics in order to mitigate dry season effects (Reiche *et al* 2018a). Forest disturbances were detected using the probabilistic algorithm described in Reiche *et al* (2018b). First, VV and VH backscatter observations were converted into forest and non-forest probabilities using pixel-specific Gaussian Mixture Models derived from the historical time-series metrics, and the larger non-forest probability was selected. An alert was triggered for non-forest probabilities >0.75. For triggered alerts, Bayesian updating (Reiche *et al* 2015) was used to calculate the forest disturbance probability and iteratively update it with the non-forest probability of later observations. Unconfirmed, low confidence alerts were provided for a forest disturbance probability >0.85. Alerts were confirmed with high confidence for forest disturbance probabilities >0.975 within a maximum period of 90 days from first detection.

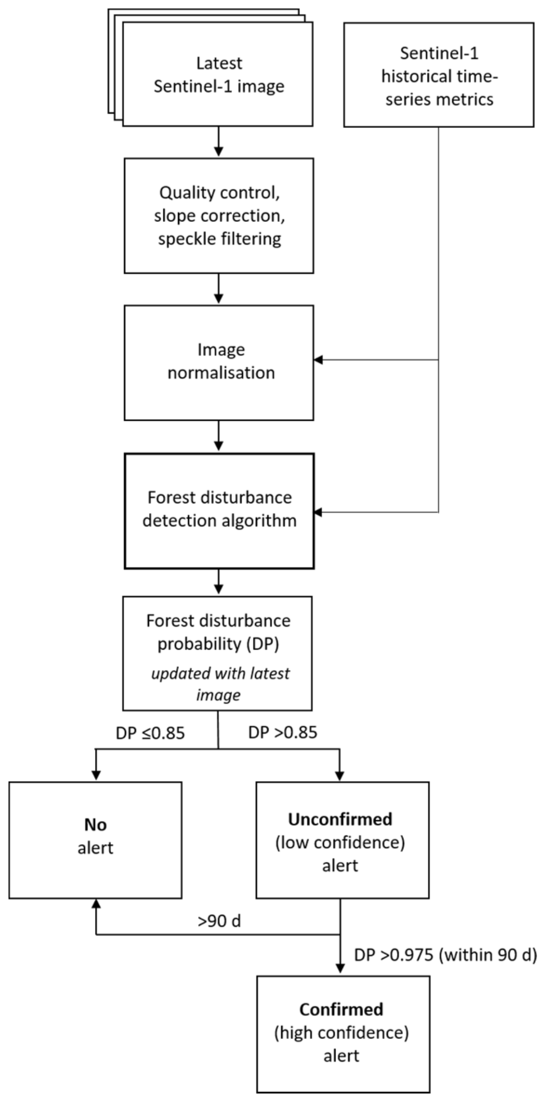

Figure 3. Flowchart of the Sentinel-1-based forest disturbance detection method.

The resulting images have a pixel size of 10 m. We clustered alert pixels in eight connected directions and removed clusters smaller than the minimum mapping unit of 0.2 ha.

4.3. Validation

We validated the Sentinel-1-based forest disturbance alert product for the year 2019 using high-resolution optical satellite data. The 2019 product was generated in an emulated near real-time mode, similar to other studies validating forest disturbance alerts (Hansen *et al* 2016, Reiche *et al* 2018a). We used probability sampling (Stehman *et al* 2003) and generated three strata with a total of 1100 sample points. We allocated 500 sample points to the stratum 'forest disturbance' to have a good estimate of the rate of false detection (commission error), important for assessing near real-time systems in particular. To target omission errors, which are more likely to occur in spatial proximity to existing forest disturbances, we allocated 300 sample points to the stratum 'No disturbance within a 20 pixel buffer zone' following Olofsson *et al* (2020). Additionally, we allocated 300 sample points to the stratum 'No disturbance outside the buffer zone'. The sampling and population unit corresponded to our 10 m × 10 m Sentinel-1 pixel (~0.01 ha).

We checked each of the sample locations for forest disturbance by visually examining monthly PlanetScope image mosaics (3 m spatial resolution) (Planet Team 2020), and supported the analysis with Sentinel-2 imagery (10 m spatial resolution). Cloud-free PlanetScope and Sentinel-2 data were infrequent in many parts of the Congo Basin, and often limited the verification process to quarterly or half-yearly time steps. In extreme cases where no cloud-free data was available during 2019, we depended on the Sentinel-1 time series imagery itself.

Our benchmark forest map relied on a Landsat-based annual tree cover loss product (Hansen *et al* 2013) to exclude forest disturbance events that occurred in 2018 and before. Some prior disturbance events were not detected by the Landsat-based algorithm, for example due to a lack of cloud-free Landsat data at the end of 2018. Disturbances detected by the Sentinel-1-based disturbance alerts in 2019 that originally occurred before 1 January 2019 (as visible in PlanetScope time series) were labelled as 'pre-2019 disturbance', but not reported as false detections (commission error).

Boundary pixels often represent partial tree cover at the edge of larger disturbance events, which makes validation ambiguous and difficult (Hansen *et al* 2016), in particular when dealing with higher spatial resolution data such as from Sentinel-1. Sample pixels that were ambiguous and that were on the boundary of larger disturbance events clearly visible in Planet imagery were labelled as 'boundary pixel', but not reported as false detections (commission error). This was done to not penalize our alerting system since the goal of alerting systems is the correct detection of new events and not the unbiased estimation of areas (Tang *et al* 2019).

In cases where a forest disturbance was visible for a sample location and not detected by our alerts (omission error), we digitized the omitted disturbance event and reported its area.

To estimate the accuracy of forest disturbance detection, we accounted for unequal inclusion probabilities between different strata as sample points were not allocated proportionally to the strata areas (Stehman *et al* 2003). Sample inclusion probability was calculated based on the number of sample points and strata areas. The estimation weights, i.e. the inverse of inclusion probability, were then used to construct an area weighted confusion matrix and calculate user's accuracy (1—false detection rate, 1—commission error) and producer's accuracy (detection rate, 1—omission error)

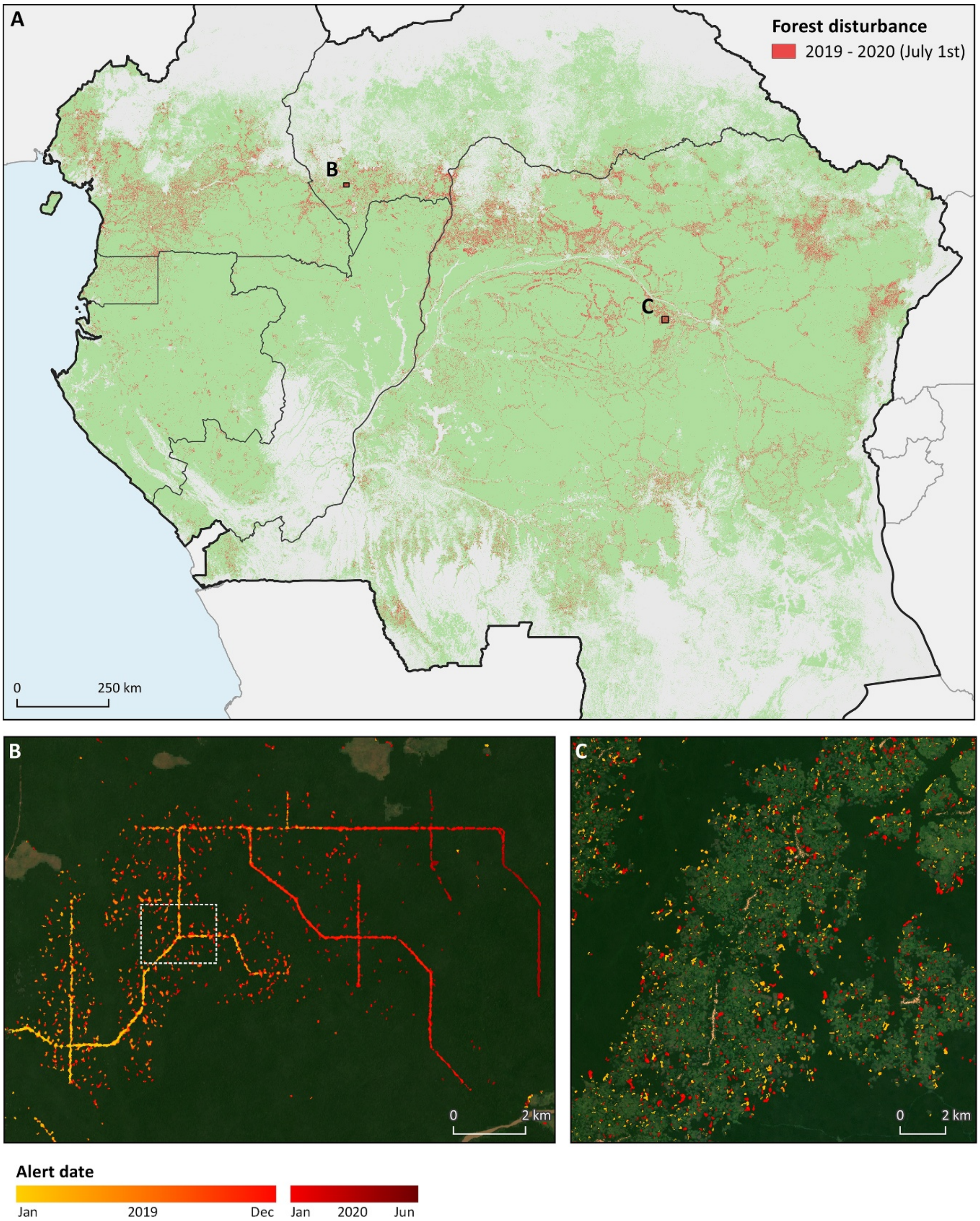

Figure 4. (A) Detected disturbance alerts for the Congo Basin's humid tropical forest for the period 2019 through to 1 July 2020. Areas indicated by B and C are shown in detail maps. Detail maps show the alert date with a Sentinel-2 composite as a base map. (B) Logging road and selective logging expansion in Sangha-Mbaéré district, Central African Republic (center coordinate: 3.95°N, 16.02°E). The white box in (B) encloses the mapped disturbance alerts for the area depicted in figure 1. (C) Smallholder agriculture in Tshopo province, Democratic Republic of the Congo (center coordinate: 0.59°N, 24.97°E).

(Stehman *et al* 2003, Stehman 2014). We excluded samples representing events <0.2 ha to estimate the producer's accuracy of our product at the applied minimum mapping unit of 0.2 ha. We used all samples to get an estimate of the producer's accuracy including disturbance events <0.2 ha which were not mapped due to the applied minimum mapping unit.

To assess the accuracy of unconfirmed alert pixels that were eventually confirmed, we calculated the total number of unconfirmed alerts throughout 2019 at four randomly selected 1° tiles. We used the resulting map from 1 July 2020 to retrieve the total number of confirmed alerts for 2019 and calculate the percentage.

For confirmed alert pixels, we assessed the time between the date when the disturbance was first detected by the algorithm and when it was confirmed (Reiche *et al* 2018b).

Table 1. Mapped forest disturbances (confirmed and unconfirmed) for the period 2019–1 July 2020 grouped by different size ranges.

Alert event size (ha)	No. Events	% Events	Area (kha)	% Area
0.2–<0.5	3238 503	79.6	469.1	32.8
0.5–<1	523 541	12.8	361.2	25.2
1–<5	295 872	7.3	502.6	35.1
⩾5	10 228	0.3	98.1	6.9
Total	4068 144	100.0	1431.0	100.0

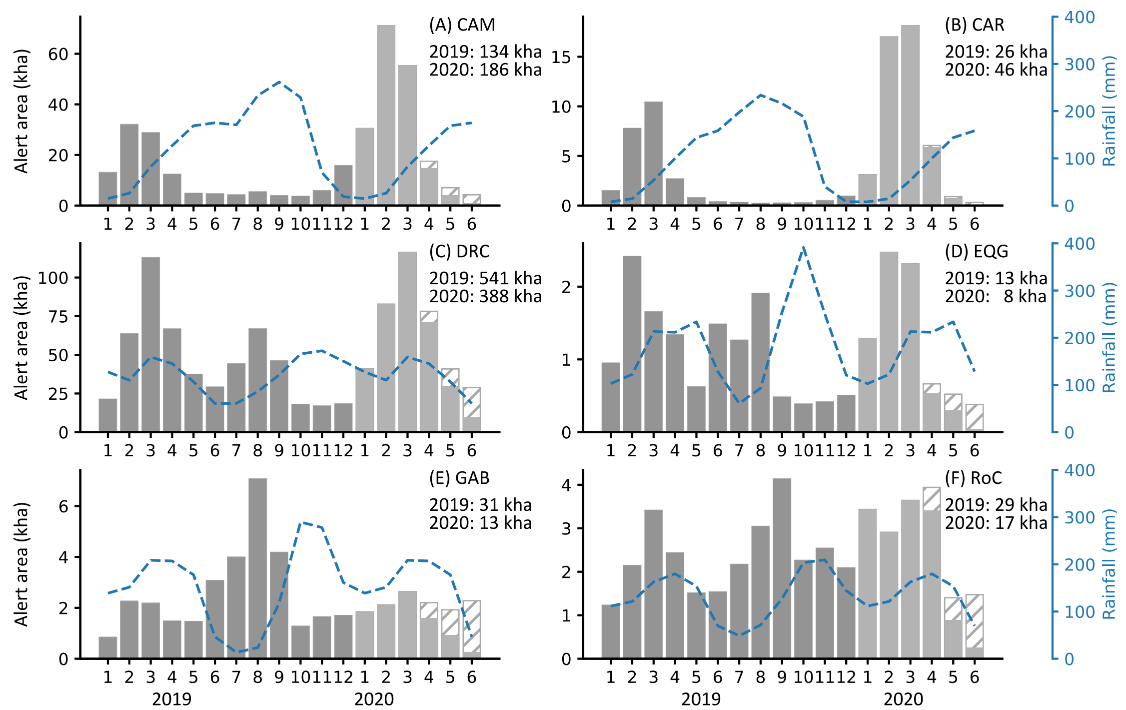

Figure 5. Monthly forest disturbance area and rainfall totals for Cameroon (A), Central African Republic (B), the Democratic Republic of the Congo (C), Equatorial Guinea (D), Gabon (E) and the Republic of the Congo (F). Rainfall data represents average monthly totals for 1991–2016 (Harris *et al* 2014). Unconfirmed alerts are indicated as bars with diagonal lines. Annual forest disturbance area is given for 2019 and 2020 individually. The year 2020 results cover the period until 1 July 2020. Note that the *y*-axes (alert area) have different ranges.

Table 2. Estimated user's accuracy (1—false detection rate) and producer's accuracy (detection rate) for confirmed alerts (% ± standard error).

User's accuracy	
Disturbances ⩾0.2 ha	97.6 ± 4.8
Producer's accuracy	
Disturbances ⩾0.2 ha	95.0 ± 25.8
All disturbances, including those smaller than the minimum mapping unit of 0.2 ha	83.5 ± 37.5

5. Results and discussion

5.1. Forest disturbance alerts

Disturbance alerts for the humid tropical forest of the Congo Basin for the period between 1 January 2019 and 1 July 2020 are depicted in figure 4. Two detail maps show the expansion of logging roads and selective logging in the Central African Republic (B), and smallholder agriculture in the Democratic Republic of the Congo (C). The white box in (B) encloses the area depicted by high-resolution PlanetScope imagery in figure 1. It shows the detection of some of the canopy openings during the short period between disturbance and canopy closure and/or understory revegetation.

While this product is designed to provide near real-time alerts and not to represent the true area of disturbances, the mapped areas can be used to evaluate relative temporal and spatial trends. We mapped 1431 kha of disturbance (of which 57 kha represented an unconfirmed alert), and a total of 4.07 million disturbance events (table 1). Forest disturbance area totals varied greatly by country. For the year 2019, for example, the mapped disturbance area totals ranged from 13 kha for Equatorial Guinea to 541 kha for the Democratic Republic of the Congo.

Small forest disturbance events dominated the detected alerts, with 79.6% of all events having a mapped size between 0.2 and <0.5 ha (32.8% of the total mapped area). We assume that many of these

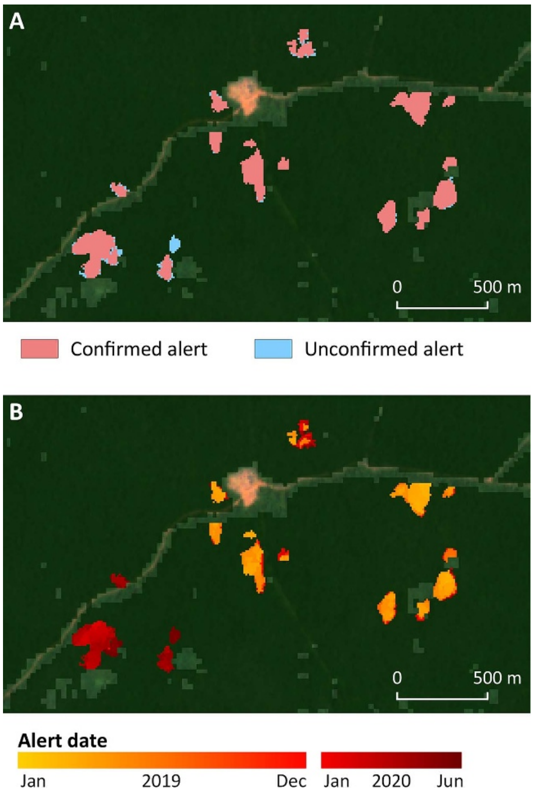

Figure 6. Delivery of the Sentinel-1-based forest disturbance alerts. Information is provided on (A) whether an alert was confirmed or is still unconfirmed at the date of the latest Sentinel-1 image, and (B) the date when the forest disturbance was first detected. The baseline forest map (opaque) is overlaid on top of a Sentinel-2 composite. (A) and (B) Show results from 1 July 2020. Location: Tshopo province, Democratic Republic of the Congo (centre coordinate: 0.09° N, 25.34° E).

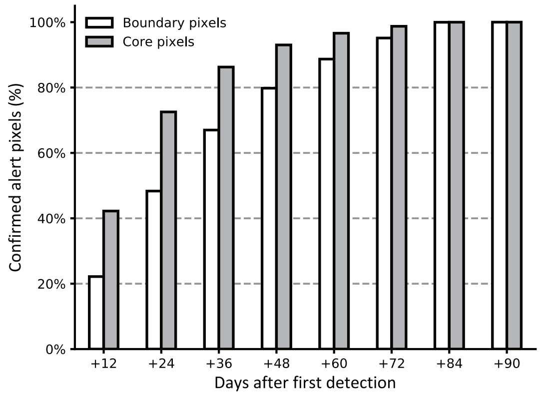

Figure 7. The number of days between the first detection and confirmation of disturbance alerts.

are related to selective logging as seen in figure 4 (B) for example. Disturbance events with a mapped size between 0.5 and <1 ha accounted for 12.8% (25.2% of the total mapped area), medium-scale events between 1 and <5 ha for 7.3% (35.1% of the total mapped area), and large-scale events ⩾5 ha for 0.3% (6.9% of the total mapped area).

The monthly distribution of forest disturbance areas shows a large variation between the six Congo Basin countries (figure 5). This can be linked to regional differences in the dry and wet season and related rainfall patterns. In general, forest disturbance rates were much higher during dry season months with low rainfall totals. Lower disturbance rates during the wet season are common in the tropics (Hansen *et al* 2016, Vargas *et al* 2019), as heavy rainfall makes many logging roads inaccessible and forest clearing operations are less feasible (Kleinschroth and Healey 2017).

The delivery of the Sentinel-1-based forest disturbance alerts is illustrated in figure 6. We provide information for each 10 m pixel within the boundary of the baseline forest map on (A) whether an alert was confirmed (high confidence alert) or is still unconfirmed (low confidence alert) at the date of the latest Sentinel-1 image, and (B) the date when the forest disturbance was first detected.

5.2. Validation results

The accuracy assessment yielded consistently high results (table 2). The user's and producer's accuracies of confirmed disturbance alerts were 97.6% and 95.0%, respectively, suggesting confident detection of forest disturbances larger than or equal to 0.2 ha. When including samples representing disturbance events <0.2 ha, the producer's accuracy was 83.5% indicating a high rate of fine-scale disturbance events which were not detected due to the application of a minimum mapping unit of 0.2 ha.

Out of the 488 correctly detected disturbance samples (out of a total of 500), 46 samples included alert detections of forest disturbance that occurred before 1 January 2019 ('pre-2019 disturbance'), but were not included in the Landsat-based tree cover loss products used to generate our benchmark forest map. We also identified 24 boundary pixels ('boundary pixel') that could not be validated unambiguously and were thus reported as correctly detected.

We examined the 12 samples labeled as commission error and identified three primary sources of false detections: dynamics in non-forested swamp and savannah areas that remained in our benchmark forest map (7 samples), swamp forest dynamics such as seasonal inundation changes that cause strong radar backscatter variations (2 samples), and unidentifiable causes of falsely detected small-scale events (3 samples). For the first source of error, false detections in non-forested land can be decreased by introducing a more accurate benchmark forest product.

The percentage of unconfirmed alerts that were eventually confirmed was found to be 62 ± 28% (% ± standard error). This means that unconfirmed alerts provide a good early indication of new disturbances, but only confirmed alerts provide high confidence information.

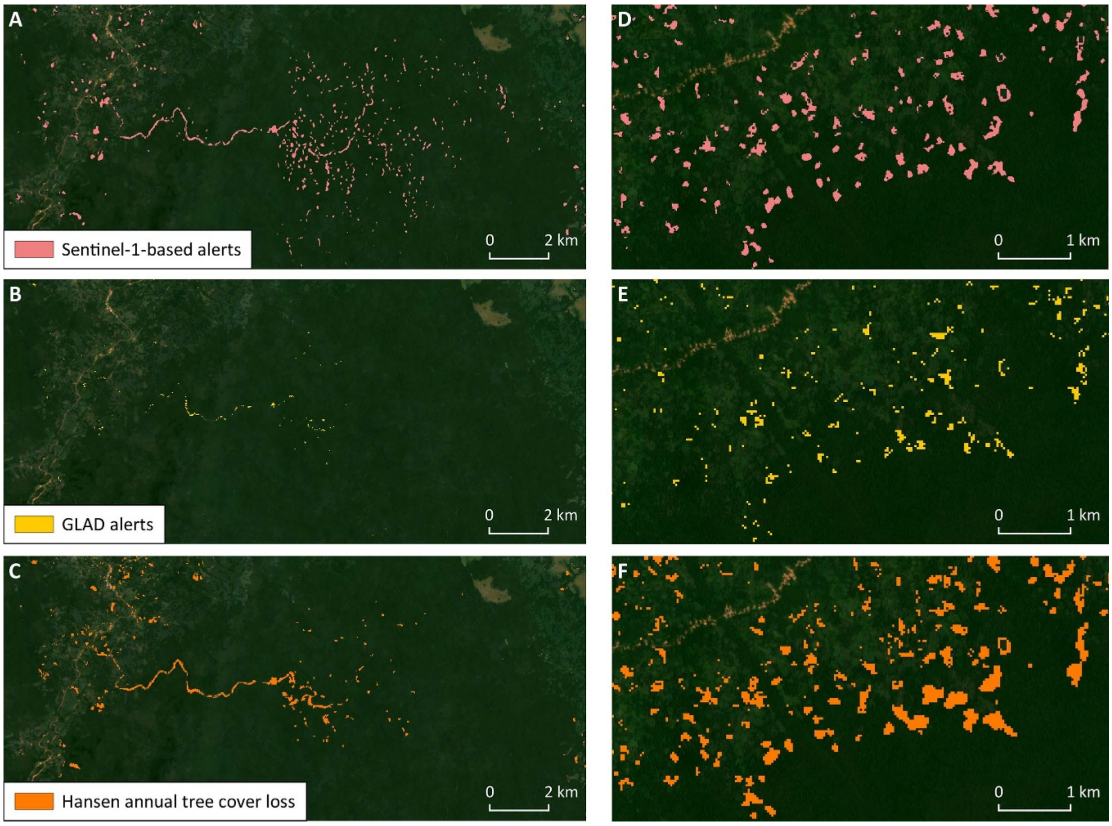

Figure 8. Visual comparison between our Sentinel-1-based alerts for 2019 with the Landsat-based GLAD alerts (Hansen et al 2016), and Landsat-based annual tree cover loss (Hansen et al 2013). The first area (A)–(C) depicts logging roads and selective logging expansion in the province Haut-Ogooué, Gabon (center coordinate: 1.68° S, 13.17° E). The second area (D)–(F) depicts smallholder agriculture in the Équateur Province, Democratic Republic of the Congo (center coordinate: 1.37° N, 20.59° E). A Sentinel-2 composite was used as base map.

Figure 7 depicts the number of days between the first detection (trigger) of a disturbance alert and its confirmation, separately for boundary and core pixels of mapped disturbance events. In general, core pixels represent complete (or close to complete) tree cover removal, and therefore the algorithm only requires a few observations to confirm core pixel with high confidence. We found 74% of all core pixels being confirmed within 24 days and 95% within 48 d. Boundary pixels, in contrast to core pixels, often represent partial tree cover removal and on average require more observations to be confirmed with high confidence. Results showed 53% of boundary pixels being confirmed within 24 days and 83% within 48 d.

We also assessed the confirmation time for different Sentinel-1 revisit times. Within 24 days, 62% of the alerts (boundary and core pixels) were confirmed for areas with a 12 days revisit time and 66% for $\leqslant$6 days revisit time. Within 48 days, 88% and 89% were confirmed for 12 days and $\leqslant$6 days revisit times, respectively.

Depending on the Sentinel-1 revisit times, the actual date on which the forest disturbance occurred is usually not more than 6–12 days before the reported date of the Sentinel-1 image that first triggered the alert (Reiche *et al* 2018b). In some circumstances, the first detection of new disturbances can be delayed due to, for example, increased soil moisture after strong rain events or remaining stems after logging, both of which can cause the Sentinel-1 C-band radar backscatter of newly disturbed areas to remain at or increase back to the level of undisturbed forest (Woodhouse *et al* 1999, Reiche *et al* 2018a).

5.3. Comparison with Landsat-based products

Compared to the GLAD alerts, which are conservative by design (Hansen *et al* 2016), our detected forest disturbance area was found to be 3 (Democratic Republic of the Congo) to 40 (Equatorial Guinea) times higher (table 3). The ratio was largest for the western Congo Basin countries of Cameroon, Equatorial Guinea and Gabon, where cloud cover is more persistent than in other parts of the Congo Basin (Tyukavina *et al* 2018). Comparison with Landsat-based annual tree cover loss showed similar magnitudes of detected disturbance areas with ratios ranging between 0.7 (Democratic Republic of the Congo) up to 1.6 (Central African Republic). The key advantage of the Sentinel-1-based alert product is its availability in near real-time.

Table 3. Mapped forest disturbance area (in kha) for the year 2019 compared for Sentinel-1-based alerts (this study), Landsat-based GLAD alerts (Hansen *et al* 2016), and Landsat-based annual tree cover loss (Hansen *et al* 2013).

	Sentinel-1-based alerts (this study)	GLAD alerts (Hansen *et al* 2016)	Annual tree cover loss (Hansen *et al* 2013)
Cameroon	134.3	6.0	86.3
Central African Republic	26.0	3.6	16.5
Democratic Republic of the Congo	541.2	179.3	827.3
Equatorial Guinea	13.4	0.3	8.3
Gabon	31.1	1.4	22.8
Republic of the Congo	28.5	4.7	41.6
Total	774.5	195.3	1002.7

Visual comparison with the GLAD alerts and Landsat-based annual tree cover loss shows the ability of our Sentinel-1-based alerts for improved detection of logging roads and selective logging as well as improved spatial detail of mapping smallholder agriculture (figure 8).

6. Conclusions

Here we present a Sentinel-1-based forest disturbance alert product for the humid tropical forest of the Congo Basin. Our disturbance alerts provide confident and rapid detection of events larger than or equal to 0.2 ha. Almost 80% of all mapped disturbance events were smaller than 0.5 ha and likely represented selective logging activities in many cases. The availability of consistent, gap-free Sentinel-1 radar observations every 6–12 days at 10 m spatial scale enabled the timely detection of such small-scale disturbances, and the confirmation of nearly all alert pixels within a few weeks after their first detection.

The new alert product helps overcome some of the data scarcity of up-to-date logging road and selective logging information in the Congo Basin region (Umunay *et al* 2019, Jackson and Adam 2020) and offers a more accurate look at the spatio-temporal forest dynamics than ever before. Results revealed a strong difference in the monthly distribution of forest disturbances across the six countries, with most disturbances occurring in the dry season month.

The primary limitations of the presented alerts are twofold. First, the high sensitivity of C-band radar to moisture variations caused a number of false alerts in swamp forests. Second, fine-scale forest disturbances <0.2 ha were not mapped due to the applied minimum mapping unit of 0.2 ha. Our results suggest that disturbance rates in the Congo Basin are therefore even higher than what was reported. In future research, we aim to decrease the minimum mapping unit, while preserving a low commission error of the alerts. The verification of fine-scale and low impact disturbances such as single tree canopy damages, however, is very challenging due to the shortage of high and very high-resolution and cloud-free reference data at weekly to monthly time steps.

This study highlights the value of Sentinel-1 dense time series data for large-area and rapid tropical forest monitoring that can be expanded to more areas in the humid tropics. The guaranteed availability of Sentinel-1 data for at least 10+ years through the upcoming Sentinel-1C and -1D satellites (Torres and Davidson 2019) provides the necessary data continuity for long term operational products. The integration with data from new high spatial and temporal resolution radar sensors, for example from the upcoming L-band NISAR (NASA/ISRO Synthetic Aperture Radar, planned launch in 2021) mission (Rosen *et al* 2016), and the integration with optical satellite data (e.g. with Sentinel-2) or products (e.g. Landsat-based GLAD alerts, Hansen *et al* 2016) offers opportunities to further improve the timeliness of confident forest disturbance alerting (Reiche *et al* 2016).

The new alert product is made available as a public good via the Global Forest Watch platform. It contributes to the efforts of Global Forest Watch to make changes in tropical forests more transparent and actionable, and provides stakeholders in the Congo Basin with improved near real-time forest disturbance information that can support their sustainable forest management and law enforcement efforts.

Data availability statement

The data that support the findings of this study are available upon reasonable request from the authors.

Acknowledgments

This project received funding through Norway's Climate and Forest Initiative (NICFI), the US Government's SilvaCarbon program, and the European Union's Horizon 2020 project 'Capacity for Copernicus REDD+ and Forest Monitoring Services (REDDCopernicus)' project (Grant Agreement No 821880). This work was also supported by the Global Forest Observation Initiative (GFOI) research and development program. PlanetScope data was provided through the Planet ambassador program. Contains modified Copernicus Sentinel data (2015–2020). We thank the two anonymous reviewers for their valuable comments.

ORCID iD

Johannes Reiche https://orcid.org/0000-0002-4327-4349

References

Asner G P, Keller M, Pereira R Jr , Zweede J C and Silva J N M 2004 Canopy damage and recovery after selective logging in Amazonia: field and satellite studies *Ecol. Appl.* **14** 280–98

Ballère M, Bouvet A, Mermoz S, Le Toan T, Koleck T, Bedeau C, André M, Forestier E, Frison P L and Lardeux C 2021 SAR data for tropical forest disturbance alerts in French Guiana: benefit over optical imagery *Remote Sens. Environ.* **252** 1–15

Bouvet A, Mermoz S, Ballère M, Koleck T and Le Toan T 2018 Use of the SAR shadowing effect for deforestation detection with Sentinel-1 time series *Remote Sens.* **10** 1250

Buchhorn M, Lesiv M, Tsendbazar N E, Herold M, Bertels L and Smets B 2020 Copernicus global land cover layers-collection 2 *Remote Sens.* **12** 1–14

Creese A, Washington R and Jones R 2019 Climate change in the Congo Basin: processes related to wetting in the December–February dry season *Clim. Dyn.* **53** 3583–602

Diniz C G *et al* 2015 DETER-B: the new Amazon near real-time deforestation detection system *IEEE J. Sel. Top. Appl. Earth Obs. Remote Sens.* **8** 3619–28

European Space Agency 2020a Sentinel-1 SAR user guide (available at: https://sentinels.copernicus.eu/web/sentinel/user-guides/sentinel-1-sar)

European Space Agency 2020b Sentinel-1 toolbox, 2020 (available at: https://sentinel.esa.int/web/sentinel/toolboxes/sentinel-1)

Finer B M, Novoa S, Weisse M J, Petersen R, Mascaro J, Souto T, Stearns F and Martinez R G 2018 Combating deforestation: from satellite to intervention *Science* **360** 1303–5

Google Earth Engine 2020 Sentinel-1 algorithms (available at: https://developers.google.com/earth-engine/sentinel1)

Gorelick N, Hancher M, Dixon M, Ilyushchenko S, Thau D and Moore R 2017 Google Earth Engine: planetary-scale geospatial analysis for everyone *Remote Sens. Environ.* **202** 18–27

Hansen M C *et al* 2013 High-resolution global maps of 21st-century forest cover change *Science* **342** 850–3

Hansen M C, Krylov A, Tyukavina A, Potapov P V, Turubanova S, Zutta B, Ifo S, Margono B, Stolle F and Moore R 2016 Humid tropical forest disturbance alerts using Landsat data *Environ. Res. Lett.* **11** 34008

Harris I, Jones P D, Osborn T J and Lister D H 2014 Updated high-resolution grids of monthly climatic observations—the CRU TS3.10 dataset *Int. J. Climatol.* **34** 623–42

Hethcoat M, Carreiras J, Edwards D, Bryant R and Quegan S 2020 Detecting tropical selective logging with SAR data requires a time series approach (bioRxiv Prepr) pp 1–33

Hirschmugl M, Deutscher J, Sobe C, Bouvet A, Mermoz S and Schardt M 2020 Use of SAR and optical time series for tropical forest disturbance mapping *Remote Sens.* **12** 1–29

Hoekman D H and Reiche J 2015 Multi-model radiometric slope correction of SAR images of complex terrain using a two-stage semi-empirical approach *Remote Sens. Environ.* **156** 1–10

Hoekman D, Kooij B, Quiñones M, Vellekoop S, Carolita I, Budhiman S, Arief R and Roswintiarti O 2020 Wide-area near-real-time monitoring of tropical forest degradation and deforestation using Sentinel-1 *Remote Sens.* **12** 3263

Jackson C M and Adam E 2020 Remote sensing of selective logging in tropical forests: current state and future directions *IForest* **13** 286–300

Joshi N *et al* 2016 A review of the application of optical and radar remote sensing data fusion to land use mapping and monitoring *Remote Sens.* **8** 70

Kleinschroth F and Healey J R 2017 Impacts of logging roads on tropical forests *Biotropica* **49** 620–35

Kleinschroth F, Laporte N, Laurance W F, Goetz S J and Ghazoul J 2019 Road expansion and persistence in forests of the Congo Basin *Nat. Sustainability* **2** 628–34

Lescuyer G, Cerutti P O, Tshimpanga P, Biloko F, Adebu-Abdala B, Tsanga R, Yembe-Yembe R I and Essiane-Mendoula E 2014 *The Domestic Market for Smallscale Chainsaw Milling in Gabon: Present Situation, Opportunities and Challenges* (Bogor, Indonesia: Center for International Forestry Research (CIFOR))

Lynch J, Maslin M, Balzter H and Sweeting M 2013 Choose satellites to monitor deforestation *Nature* **496** 293–4

Martone M, Rizzoli P, Wecklich C, González C, Bueso-Bello J L, Valdo P, Schulze D, Zink M, Krieger G and Moreira A 2018 The global forest/non-forest map from TanDEM-X interferometric SAR data *Remote Sens. Environ.* **205** 352–73

Olofsson P, Arévalo P, Espejo A B, Green C, Lindquist E, McRoberts R E and Sanz M J 2020 Mitigating the effects of omission errors on area and area change estimates Mitigating the effects of omission errors on area and area change estimates *Remote Sensing of Environment* **236** 111492

Planet Team 2020 Planet application program interface: in space for life on Earth (availble at: https://api.planet.com)

Potapov P V, Turubanova S A, Hansen M C, Adusei B, Broich M, Altstatt A, Mane L and Justice C O 2012 Quantifying forest cover loss in Democratic Republic of the Congo, 2000–2010, with Landsat ETM+ data *Remote Sens. Environ.* **122** 106–16

Potin P, Rosich B, Miranda N and Grimont P 2016 Sentinel-1 mission status *Procedia Comput. Sci.* **100** 1297–304

Quegan S and Yu J J 2001 Filtering of multichannel SAR images *IEEE Trans. Geosci. Remote Sens.* **39** 2373–9

Reiche J *et al* 2016 Combining satellite data for better tropical forest monitoring *Nat. Clim. Change* **6** 120–2

Reiche J, de Bruin S, Hoekman D H, Verbesselt J and Herold M 2015 A Bayesian approach to combine Landsat and ALOS PALSAR time series for near real-time deforestation detection *Remote Sens.* **7** 4973–96

Reiche J, Hamunyela E, Verbesselt J, Hoekman D and Herold M 2018a Improving near-real time deforestation monitoring in tropical dry forests by combining dense Sentinel-1 time series with Landsat and ALOS-2 PALSAR-2 *Remote Sens. Environ.* **204** 147–61

Reiche J, Verhoeven R, Verbesselt J, Hamunyela E, Wielaard N and Herold M 2018b Characterizing tropical forest cover loss using dense Sentinel-1 data and active fire alerts *Remote Sens.* **10** 1–18

Rosen P, Hensley S, Shaffer S, Edelstein W, Kim Y, Kumar R, Misra T,, Bhan R, Satish R and Sagi R 2016 An update on the NASA-ISRO dual-frequency DBF SAR (NISAR) mission *Int. Geosci. Remote Sens. Symp.* (*November 2016 Beijing, China* IEEE) pp 2106–8

Sannier C, Mcroberts R E, Fichet L-V and Makaga E M K 2014 Using the regression estimator with Landsat data to estimate proportion forest cover and net proportion deforestation in Gabon *Remote Sens. Environ.* **151** 138–48

Somorin O A, Peach H C, Visseren-hamakers I J and Sonwa D J 2012 The Congo Basin forests in a changing climate: policy discourses on adaptation and mitigation (REDD+) *Glob. Environ. Change* **22** 288–98

Souza C M, Siqueira J V, Sales M H, Fonseca A V, Ribeiro J G, Numata I, Cochrane M A, Barber C P, Roberts D A and Barlow J 2013 Ten-year landsat classification of deforestation and forest degradation in the Brazilian Amazon *Remote Sens.* **5** 5493–513

Souza C, Roberts D and Cochrane M 2005 Combining spectral and spatial information to map canopy damage from selective logging and forest fires *Remote Sens. Environ.* **98** 329–43

Souza J C M, Hayashi S and Verissimo A 2009 Near real-time deforestation detection for enforcement of forest reserves in Mato Grosso *L. Gov. Support MDGS Responding to new challenges* (*2008*) pp 1–8 (https://www.fig.net/resources/proceedings/2009/fig_wb_2009/papers/trn/trn_2_souza.pdf)

Stehman S V 2014 Estimating area and map accuracy for stratified random sampling when the strata are different from the map classes *Int. J. Remote Sens.* **35** 4923–39

Stehman S V, Wickham J D, Smith J H and Yang L 2003 Thematic accuracy of the 1992 National Land-Cover Data for the eastern United States: statistical methodology and regional results *Remote Sens. Environ.* **86** 500–16

Tabor K M and Holland M B 2020 Opportunities for improving conservation early warning and alert systems *Remote Sens. Ecol. Conserv.* **6** 1–11

Tang X, Bullock E L, Olofsson P, Estel S and Woodcock C E 2019 Near real-time monitoring of tropical forest disturbance: new algorithms and assessment framework *Remote Sens. Environ.* **224** 202–18

Torres R *et al* 2012 GMES Sentinel-1 mission *Remote Sens. Environ.* **120** 9–24

Torres R and Davidson M 2019 Overview of Copernicus SAR space component and its evolution *IEEE Int. Geosci. Remote Sens. Symp.* (Yokohama, Japan: IEEE) pp 5381–4

Tyukavina A, Hansen M C, Potapov P, Parker D, Okpa C, Stehman S V, Kommareddy I and Turubanova S 2018 Congo Basin forest loss dominated by increasing smallholder clearing *Sci. Adv.* **4** eaat2993

Ulaby T F, Moore R K and Fung A K 1986 *Microwave Remote sensing—Active and Passive* (Norwood, MA: Artech House)

Umunay P M, Gregoire T G, Gopalakrishna T, Ellis P W and Putz F E 2019 Selective logging emissions and potential emission reductions from reduced-impact logging in the Congo Basin *For. Ecol. Manage.* **437** 360–71

Vargas C, Montalban J and Leon A A 2019 Early warning tropical forest loss alerts in Peru using Landsat *Environ. Res. Commun.* **1** 121002

Verhegghen A, Eva H and Achard F 2015 Assessing forest degradation from selective logging using time series of fine spatial resolution imagery in Republic of Congo *Int. Geosci. Remote Sens. Symp.* (*November 2015 Milan, Italy* IEEE) pp 2044–7

Vollrath A, Mullissa A and Reiche J 2020 Angular-based radiometric slope correction for Sentinel-1 on Google Earth Engine *Remote Sens.* **12** 1–14

Watanabe M, Koyama C N, Hayashi M, Nagatani I and Shimada M 2018 Early-stage deforestation detection in the tropics with L-band SAR *IEEE J. Sel. Top. Appl. Earth Obs. Remote Sens.* **11** 2127–33

Weisse M J, Noguerón R, Vivianco Vincencio R E and Castillo Soto D A 2019 Use of near-real-time deforestation alerts: a case study from Peru World Resources Institute (https://files.wri.org/s3fs-public/use-near-real-time-deforestation-alerts.pdf)

Woodhouse I, van der Sanden J J and Hoekman D H 1999 Scatterometer observations of seasonal backscatter variation over tropical rain forest *IEEE Trans. Geosci. Remote Sens.* **37** 859–61

Danklmayer A, Doring B, Schwerdt M and Chandra M 2009 Assessment of Atmospheric Propagation Effects in SAR Images Assessment of Atmospheric Propagation Effects in SAR Images *IEEE Trans. Geosci. Remote Sensing* **47** 3507–18